IOP Conf. Series: Materials Science and Engineering **397** (2018) 012059 doi:10.1088/1757-899X/397/1/012059

Theoretical and experimental analysis of photovoltaic-electrostatic driving flexible cantilever beam

Yusong Chen, Xinjie Wang, Kun Qiao and Yafeng Liu

School of Mechanical Engineering, Nanjing University of Science and Technology, Nanjing 210094,China
Email:xjwang@njust.edu.cn

Abstract. A model of photovoltaic-electrostatic driving flexible cantilever beam based on PLZT ceramic is proposed in this paper. New equivalent electrical model of PLZT ceramic connected to a parallel plate composed of two copper foils is obtained by modifying the original PLZT equivalent electrical model. After that, the mechanicalmodel of photovoltaic-electrostatic driving cantilever beam is established. Furthermore, the influences of UV light intensity on the deflection of the photovoltaic-electrostatic cantilever beam are analysed via the theoretical and experimental method. The analysis results indicate that the deflection at the end of cantilever beam increases with the increase of light intensity.

1. Introduction

Micro-cantilever beam is a very common structure in micro-mechanical system, it is commonly used in inertial sensors and actuators. The common driving methods are electrostatic drive, thermal drive, electromagnetic drive and piezoelectric drive. Because of its simplicity and low power consumption, electrostatic drive is the most widely used in micro-mechanical system. However, the traditional electrostatic drive powered by an external power supply is susceptible to electromagnetic interference. In the clean operating space and vacuum, traditional electrostatic drive has great limitations. With the development of smart materials, the emergence of new type of actuators and the breakthrough in key technology has been greatly promoted. Lead lanthanum zirconate (PLZT) ceramic can generate kV voltage between the two electrodes when exposed to 365 nm UV light, so that UV light can be used instead of an external power source as a driving source. Compared with the driving mode of the external power supply, the light driving technology has the advantages of clean driving, no electromagnetic interference, non-contact remote light control and wireless energy transmission, it is an ideal driving mode of cantilever beam.

In the past few decades, many scholars conducted a series of researches on the theory and engineering application of PLZT ceramic. In 1979, Fridkin [1] proposed the RC electrical model of PLZT ceramic along the polarization direction. In 2000, Poosanaas et al [2] pointed out that the optical secondary nonlinearity is an important cause of the anomalous photovoltaic effect. In the 1980s, Uchino et al [3] designed the photo-driven relay and the photo-driven micro-walking machine based on the photostrictive effect of the PLZT bimorph. In 1996, Tzou et al [4] proposed a two-dimensional photostrictive actuator and applied it in vibration control for rectangular plate. In 2004, Ichiki et al [5] designed an electrostatic-optical motor based on the photovoltaic effect of PLZT. In 2005, Shih et al [6] investigated a photostrictive constitutive model of PLZT with coupling opto-piezo-thermo-elastic fields. In 2007, Li et al [7] designed a light-controlled servo system and pointed out that improving the response speed of PLZT is the key to promote its engineering application. In 2009, Tong and Luo et al [8] applied 0-3 polarized PLZT ceramic to the active control of the photoelectric laminated beam. In

Content from this work may be used under the terms of the Creative Commons Attribution 3.0 licence. Any further distribution of this work must maintain attribution to the author(s) and the title of the work, journal citation and DOI.
Published under licence by IOP Publishing Ltd

2011, they studied shape morphing of laminated composite structures with photostrictive actuators via topology optimization [9]. Zheng et al [10] conducted a coupled multi-physics modeling of 0-3 polarized PLZT ceramic and carried out the finite element simulation. Huang [11] carried out the experiments on the response characteristics of PLZT ceramic, etc.

For the photovoltaic effect of PLZT ceramic, many scholars have studied the theory and applied it to active shape and vibration control of beam, plate and shell structure. Shih et al [6] combined the experimental data of Fukuda et al to deduce the constitutive equations of PLZT ceramic in 2005, but failed to consider the effect of thermal expansion on the photo-induced electric field. In 2015, Huang and Wang et al [12] considered the effect of thermal expansion on the photo-induced electric field and proposed a model for predicting photo-induced voltage and photo-induced deformation based on the coupling of multiple fields. In 2011, Rahman and Nawaz [13] carried out modeling analysis of optical actuator based on PLZT ceramic. Zheng et al [14, 15] conducted the active vibration control of photostrictive thin cylindrical shells structure. Jiang et al [16] investigated the vibration control of cylindrical shells with a hybrid photovoltaic/piezoelectric actuation mechanism. Wang et al [17] proposed closed-loop control of cantilever beam based on hybrid photovoltaic/piezoelectric actuation mechanism. These studies provide a theoretical fundament for the photovoltaic-electrostatic driving on basis of PLZT ceramic.

In this paper, the equivalent electrical model of PLZT ceramic with external load is deduced, and the mechanics model of photovoltaic-electrostatic driving cantilever beam via the micro-element method is obtained. Then, the relationship between the PLZT photovoltage and the deflection at the end of cantilever beam is investigated. After that, the theoretical analysis of the influence factors on the deflection of the cantilever beam is carried out. Finally, the established mathematical model and theory are verified through experiments.

2. Mathematical Modelling of the Photovoltaic-Electrostatic Driving Cantilever Beam based on PLZT Ceramic

2.1. Photovoltaic-Electrostatic Driving Cantilever Beam Structure

Photovoltaic-electrostatic driving cantilever beam structure is illustrated in Figure 1. It consists of PLZT ceramic photoelectric transducer, ultraviolet light source, noncontact displacement sensor, high impedance electrostatic voltmeter, flexible cantilever beam and computer.

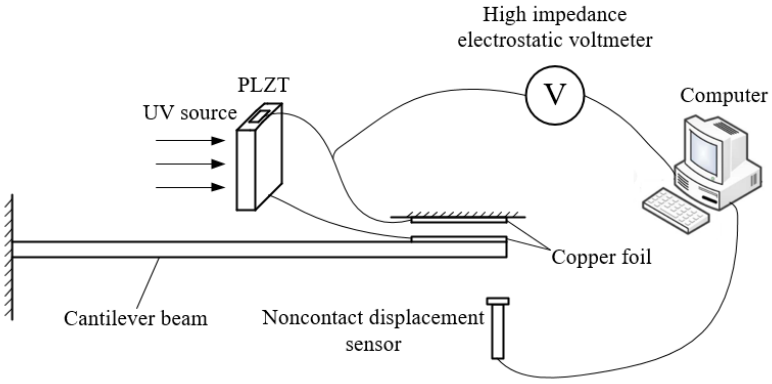

Figure 1. The schematic diagram of the photovoltaic-electrostatic driving cantilever beam

When PLZT ceramic is irradiated vertically by the ultraviolet light with a wavelength near 365 nm, the photo-generated carriers flow along the polarized direction, so that the positive electrode and the negative electrode of the PLZT ceramic collect the positive and negative charges respectively to generate a high photovoltaic voltage of several kV/cm. The silver wire is used to connect the electrodes of the PLZT ceramic to the two pieces of copper foil which are attached to the cantilever beam and the fixed base respectively with the insulating adhesive. Because the two pieces of copper

foil collect the same amount of charge respectively with the opposite polarity, the two copper foils attract each other under the action of electrostatic force to generate a driving force, thereby causing deflection of the cantilever beam.

2.2. Mathematical Modelling of the Photovoltaic-Electrostatic Driving Cantilever Beam

When a PLZT ceramic is irradiated by ultraviolet light, high photovoltaic voltage is generated between the electrodes of the ceramic, as a result of the anomalous photovoltaic, pyroelectric, photothermal and piezoelectric effects. The photovoltage responds dynamically with illumination time until it reaches saturated voltage. At this time, the PLZT ceramic can be considered as a parallel circuit consisting of a photo-current, a photo-resistor R_P and a capacitor C_P, The photovoltage between the electrodes of PLZT ceramic can be written as:

$$U_d = I_P R_P (1 - e^{-\frac{t}{R_P C_P}}) = U_s (1 - e^{-\frac{t}{\tau}}) \tag{1}$$

where I_P is photo-current; I_R is the current flowing through the resistor; I_C is the current flowing through the capacitor; τ is time constant; Us is saturated photovoltaic voltage.

When the two electrodes of the PLZT ceramic are connected to a parallel plate composed of two pieces of copper foil, part of the photo-generated carriers are conducted between the copper foils using air as a medium, and part of them are stored on the two copper foils in the form of charges. Hereby, equivalent electrical model of electrostatic parallel plate driven by PLZT ceramic is presented in Figure 2. R_a and C_a are the resistance and capacitance of the parallel plate generated by two parallel copper foils respectively.

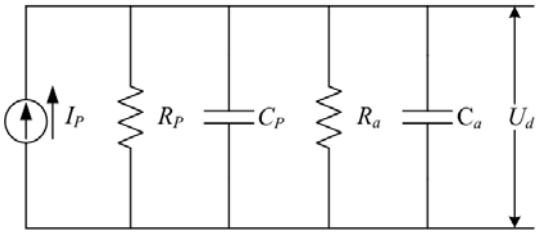

Figure 2. Equivalent electrical model of electrostatic parallel plate driven by PLZT ceramic

According to the new equivalent circuit model above, the driving voltage produced by PLZT ceramic for electrostatic parallel plate is:

$$U_d = I_P \frac{R_P \cdot R_a}{R_P + R_a} (1 - e^{-\frac{t}{\tau'}}) = U_s' (1 - e^{-\frac{t}{\tau'}}) \tag{2}$$

where τ' is the new time constant, the expression is:

$$\tau' = \frac{R_P \cdot R_a}{R_P + R_a} (C_P + C_a) \tag{3}$$

Assuming the length, width and thickness of the cantilever beam are *l*, *b* and *h*, respectively. While assuming the length and width of the copper foil arel_{cu} and b_{cu} (b_{cu} =*b*), respectively. The thickness of the copper foil is negligible herein.

Take an infinitesimal dx of cantilever beam as shown in Figure 3, it can be approximated as a micro-parallel plate capacitor in this situation. *d* is the initial distance between the two copper foils, d*w* is the deflection at the infinitesimal d*x* of cantilever beam.

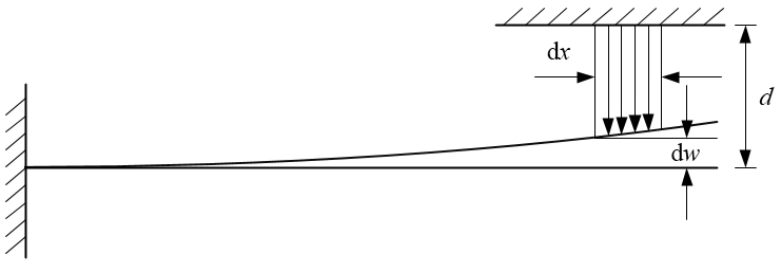

Figure 3. The schematic diagram of infinitesimal dx of cantilever beam

The internal energy of this micro-parallel plate is obtained as:

$$\mathrm{d}W = \frac{1}{2}U^2\mathrm{d}C = \frac{1}{2}U^2\frac{\varepsilon_A b_{cu}}{d-\mathrm{d}w}\mathrm{d}x \tag{4}$$

where ε_A is the dielectric constant of air; dC is the capacitance of the micro-parallel plate; U is the voltage between the two plates of the micro-capacitor.

Based on the principle of virtual work, the infinitesimal electrostatic force of the micro-parallel plate capacitor can be presented as:

$$\mathrm{d}F = \frac{\partial(\mathrm{d}W)}{\partial(\mathrm{d}w)} = \frac{1}{2}\frac{\varepsilon_A b_{cu}U^2}{(d-\mathrm{d}w)^2}\mathrm{d}x \tag{5}$$

The deflection at any point of the cantilever beam when subjected to force F is given:

$$\begin{cases} w = \dfrac{Fx^2}{6YI}(3a-x)[0 \le x \le a] \\ w = \dfrac{Fa^2}{6YI}(3x-a)[a \le x \le l] \end{cases} \tag{6}$$

where a is the distance between the point of force F and the fixed end of the cantilever beam; Y is the Young's modulus of the cantilever beam; $I$is the inertia moment of the cantilever beam.

For $x = l$, that is the free end of cantilever beam, when subjected to infinitesimal electrostatic force dF generated by infinitesimal dx, the deflection at the end of cantilever beam dw_{tail} can be written as:

$$\mathrm{d}w_{tail} = \frac{\mathrm{d}F \cdot a^2}{6YI}(3l-a) \tag{7}$$

Substituting equation (5) into equation (7), one can get another expression of the deflection at the end of cantilever beam dw_{tail}. Replacing the deflection dw of the infinitesimal dx at any position of cantilever beam with the deflection w_{tail} at the end of cantilever beam gives simplified equation as:

$$\mathrm{d}w_{tail} = \frac{1}{12YI}\frac{\varepsilon_A U^2 b_{cu}}{(d-w_{tail})^2}a^2(3l-a)\mathrm{d}x \tag{8}$$

Equation (8) shows that the deflection at the end of cantilever beam due to an infinitesimal electrostatic force dF acting on the $x = a$ of cantilever beam. For the entire cantilever beam, numerous infinitesimal parallel plate capacitors which have their own infinitesimal electrostatic forces dF together to make the end of cantilever beam generate bending deformation. The deflection at the end of cantilever beam generated by each infinitesimal electrostatic force dF satisfies the equation (7). The analytical solution of the deflection can be obtained by using the superposition property.

Replacing a by x yields the relationship between the position of infinitesimal electrostatic force dF and the corresponding dw_{tail}, as shown:

$$\mathrm{d}w_{tail} = \frac{1}{12YI}\frac{\varepsilon_A U^2 b_{cu}}{(d - w_{tail})^2} x^2(3l - x)\mathrm{d}x \tag{9}$$

According to sort out the equation (10), differential equation about cantilever beam driven by electrostatic force can be obtained. Integrating the two sides of the equation respectively generates an integral equation as:

$$\int_0^{w_{tail}} 12(d - w_{tail})^2 YI\mathrm{d}w_{tail} = \int_{l-l_{cu}}^{l} \varepsilon_A b_{cu} U^2(3lx^2 - x^3)\mathrm{d}x \tag{10}$$

Considering the boundary conditions: w_{tail}= 0 when l_{cu} = 0, the deflection w_{tail}at the end of cantilever beam can be rewritten as:

$$w_{tail} = \sqrt[3]{\frac{\varepsilon_A b_{cu} U^2}{4YI}(2l^3 l_{cu} - 1.5l^2 l_{cu}^{\ 2} + 0.25 l_{cu}^{\ 4}) - d^3} + d \tag{11}$$

Substituting equation (2) into equation (11), the relationship between the PLZT photovoltaic voltage and the deflection at the end of cantilever beam can be rewritten as:

$$w_{tail} = \sqrt[3]{\frac{\varepsilon_A b_{cu}(I_P \frac{R_P \cdot R_a}{R_P + R_a}(1 - e^{-\frac{t}{\tau'}}))^2}{4YI}(2l^3 l_{cu} - 1.5l^2 l_{cu}^{\ 2} + 0.25 l_{cu}^{\ 4}) - d^3} + d \tag{12}$$

It can be seen from equations (11) and (12) that the deflection w_{tail}at the end of cantilever beam is related to the driving voltage U_d produced by PLZT ceramic, the material parameters Y and I of the cantilever beam, the length l of the cantilever beam, the dielectric constant ε_A of air, the distance d between the two copper foils and the length l_{cu}, width b_{cu} of the copper foil.

3. Influence of Ultraviolet Light Intensity on the Deflection at the End of Cantilever Beam

The size of the PLZT sample used in this experiment is 10 mm (L_P) × 5 mm (W_P) × 1 mm (T_P). The cantilever beam is made of PMMA and has dimensions of 100 mm (L) × 5 mm (W) × 1 mm (T), Young's modulus of it is 3GPa.

Measurement diagram shown in Figure 4. When irradiated by UV light, PLZT ceramic generates photovoltage on basis of the anomalous photovoltaic effect. With the influence of the electrostatic force between the two copper foils, the deflection of the cantilever beam is generated, which is measured by a noncontact displacement sensor (STIL Initial 12), whose axial resolution with average 10 and the max linearity error are 500 nm and 180 nm, respectively. Meanwhile the voltage between the two copper foils is measured by a high impedance electrostatic voltmeter (Trek Model: 821HH), whose measurement range is 0 to ±2 kV DC and the accuracy is better than ±1% of full scale at the voltage monitor output.

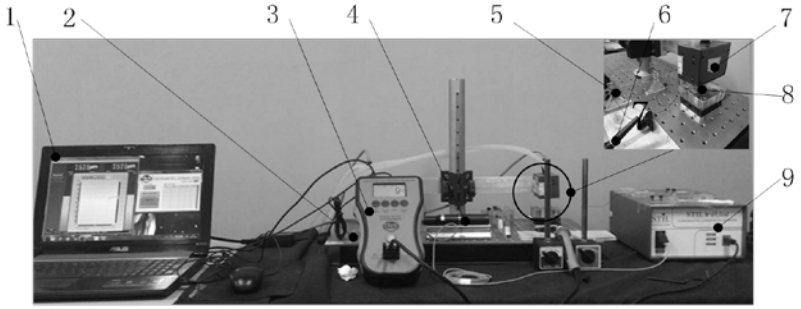

(1) PC, (2) Optical experiment platform, (3) High impedance electrostatic voltmeter, (4) Probe of displacement sensor, (5) Flexible cantilever beam, (6) Probe of high impedance electrostatic voltmeter, (7) UV light source (8) PLZT ceramic, (9) Controller of noncontact displacement sensor

Figure 4. Experimental platform of photoelectric electrostatic driving flexible cantilever beam

It can be seen from the relevant reference that when the size of PLZT ceramic is unchanged, the number of photo-generated carriers within the PLZT ceramic will increase with the light intensity increases. The macroscopic appearance is photo-current I_P increases [2]. The relationship between photo-current and ultraviolet light intensity can be described as:

$$I_P = A_{cur} I^{\alpha_{cur}} \tag{13}$$

where A_{cur} is the photo-current coefficient, α_{cur} is the photo-current constant which can be identified by experiments, and I is the light intensity.

When the PLZT ceramic is connected to the parallel plate structure, according to the equivalent electrical model of Figure 2, it shows that the saturated driving voltage of PLZT ceramic is still determined by the product of the photo-current I_P and equivalent resistance $\frac{R_P \cdot R_a}{R_P + R_a}$. Therefore, when other conditions remain unchanged, the greater the ultraviolet light intensity, the corresponding saturated driving voltage of PLZT greater.Referring to equation (11), the greater the driving voltage *U*, the corresponding deflection at the end of cantilever beam is greater.

In the experiment, the distance between the copper foils *d* is 4 mm, the length l_{cu} and the width b_{cu} of the copper foil is20 mm and 5 mm respectively. When the UV light intensity is 50, 100mW / cm^2, the curves of the photovoltaic voltage without and with copper foil load and with load varies with time are tested respectively as shown in Figure 5. It can be seen from Figure 5 that as the UV light intensity gradually increases from 50mW / cm^2 to 100mW / cm^2, both the photovoltaic voltage without and with the load increases. However, the photovoltaic voltage with load slightly lower than that without load, the trend is basically the same. This is due to the resistance R_a of the parallel copper foil is about $8\times10^{14}\Omega$ calculated based on the dimensions of the two copper foil and the air conductivity of 5×10^{-14}S / m, which is larger than the PLZT photo-resistor R_P (about $10^{12}\Omega$~$10^{13}\Omega$). Depending on the characteristics of the parallel circuit shown in Figure 2, the saturated photovoltaic voltage with load $U_s' = I_P \frac{R_P \cdot R_a}{R_P + R_a}$ will be slightly less than the saturated photovoltaic voltage without load $U_s = I_P R_P$.

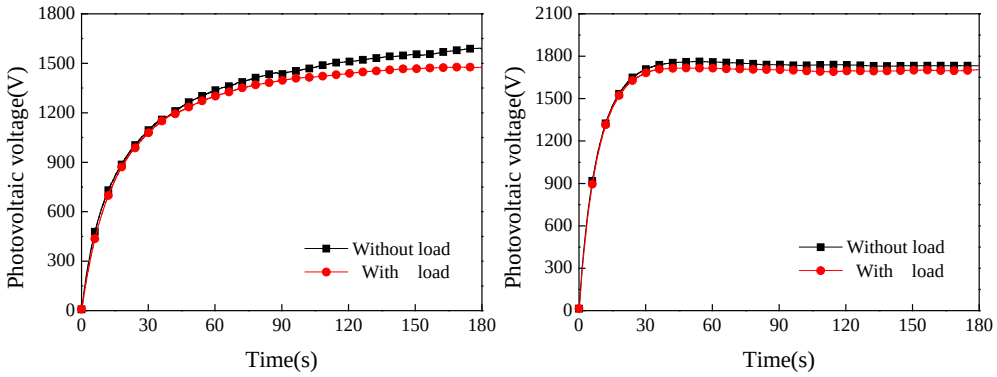

(a) Light intensity is 50mW/cm^2 (b) Light intensity is 100mW/cm^2

Figure 5. Comparison of photovoltaic voltage without and with load under various light intensities

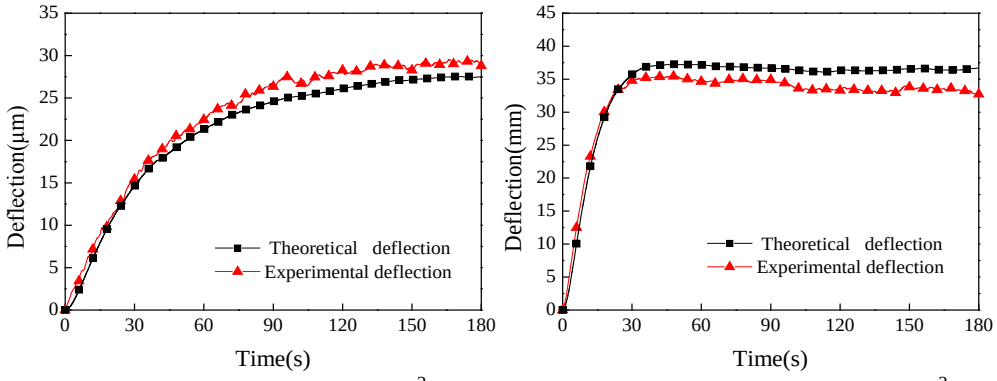

(a) Light intensity is 50mW/cm^2 (b) Light intensity is 100mW/cm^2

Figure 6. Comparisons of theoretical and experimental deflections with various light intensities

Comparisons between the theoretical and the experimental deflection curves are obtained in Figure 6. As can be seen from Figures 1 and 6, the voltage measured by the high impedance electrostatic voltmeter is actually generated by the charge accumulated on one of the two copper foils. Therefore, the driving voltage measured by the high impedance electrostatic voltmeter should be doubled and then substituted into equation (11) to get theoretical values. Comparisons between the theoretical and the experimental deflection curves are obtained in Figure 6. It can be seen from Figure 6 that the theoretical deflection curves meet well with the experimental deflection curves measured experimentally, and both increase with the increase of UV light intensity.

4. Conclusions

In this paper, a new type of photoelectric and electrostatic driving method based on PLZT ceramic is proposed. By modifying the equivalent electrical model of PLZT ceramic, a new equivalent electrical model with parallel plate capacitor was obtained. The electrostatic driving mechanics model of cantilever beam is deduced, and then the relationship between the PLZT ceramic photovoltaic voltage and the deflection at the end of cantilever beam is established.

Under the premise of other conditions remain unchanged; the deflection at the end of cantilever beam will increase with the increase of light intensity. The rationality of the model and the theoretical formula is verified by comparing theoretical deflection curve and experimental deflection curve under the light intensity of 50, 100mW/cm^2 respectively.

Acknowledgments

The authors gratefully acknowledge the funding support from the National Natural Science Foundation of China (No.51675282) and Jiangsu Overseas Visiting Scholar Program for University.

References

[1] Fridkin V M 1979 *Photoferroelectrics* (New York: Springer).
[2] Possanaas P, Tonooka KandUchino K 2000 *Mechatronics***10** 467-487.
[3] Uchino K1987*Journal of ceramic Society of Japan* **95** 545-550.
[4] Tzou H S1996 *Smart Materials & Structure* **5** 230-235.
[5] Ichiki M 2004 *Journal of the European Ceramic Society* **24** 1709-14.
[6] Shih H R, Tzou H S and Saypuri M 2005 *Journal of Sound and Vibration* **284** 361-378.
[7] Li Q, Wang S P and Liang L 2007 *Piezoelectrics &Acoustooptics* **29** 213-215.
[8] Luo Q and Tong L 2009 *International Journal of Solids and Structures* **46** 4313-21.
[9] Luo Zet al 2011 *Composite Structure* **93** 406-418.
[10] Zheng S J 2015 *Scinence China Technological Sciences* **55** 709-716.
[11] Wang X J, Huang J H and Wang J 2015 *Smart Materials & Structures* **24** 075017.
[12] Huang J H, Wang X JandWang J 2015 *Optics and Precision Engineering* **23** 760-768.
[13] Rahman M and Nawaz M 2011 *Smart Materials & Structures* **20** 115013.
[14] He R, Zheng S and TongL 2016 *Journal of Vibration and Acoustics* **138** 041003.
[15] He R and Zheng S 2014 *International Journal of Applied Electromagnetics and Mechanics* **46** 951-963.
[16] Jiang J et al 2014 *International Journal of Applied Electromagnetics & Mechanics* **46** 917-926.
[17] Wang X J, Lu F and Qiao K 2017 *International Journal of Applied Electromagnetics and Mechanics* **53** 497-509.